

THE INFLUENCE OF CYCLIC EFFORTS ON TITANIUM IMPLANTS' MECHANICAL PROPERTIES

Adrian VOICU¹, Viorel Aurel ȘERBAN¹, Aurel RĂDUȚĂ¹, Mihaela POPESCU¹,
Camelia DEMIAN¹, Bogdan TITA²

¹ University POLITEHNICA of Timisoara, Department of SMS

² UMF Timisoara, Department of Analytical Chemistry

e-mail: ¹ adrian.voicu@mec.upt.ro ; ² bogdantita@yahoo.com

Keywords: *Titanium implants, cyclic efforts, corrosion rate, biocompatibility*

Abstract: *This article studies Titanium implants behaviour under cyclic efforts influence, concerning its corrosion rate and subsequently the biocompatibility. The equipments utilised for these experiments were the Multitest 5i and Volta lab 20.*

The final results confirmed that cyclic effort, similar to those occurring in human body during mastication process, are increasing the corrosion rate and can negatively influence the biocompatibility.

1. GENERAL ASPECTS

The cranio – maxilo facial implants kit was designated to surgically resolve the complicate fractures of the skull, and also for the facial reconstruction.

2. TITANIUM'S BEHAVIOUR AS SURGICAL IMPLANT

The evaluation of mechanical behaviour of tested surgical implants was made with the help of Multitest 5i equipment (figure 1).

It is a system built for traction, compressing and bending testing, completely controlled by the computer.



Fig. 1 MultiTest 5-i equipment

For a practical demonstration of titanium's special qualities, seven surgical plates type P6, belonging to the maxilo - facial implants kit, were tested concerning their behaviour at cyclic sollicitation, and also their corrosion behaviour.

It was evaluated the way how the cyclic traction efforts are influencing the properties of the studied implants, concerning the corrosion behaviour (and implicit the biocompatibility)

Six PD6 type implants were the subject of a different number of cyclic traction efforts, ranging between 0-400, and the increment rate being of 100 cycles.

After that, the implants were the subjects of corrosion rate evaluation, by electrochemical methods, as it can be seen in table 1.

Table 1 The number of cyclic solicitations

Nr.	Nr. of cyclic solicitations	Corrosion
1	0	NO
2	0	YES
3	100	YES
4	200	YES
5	300	YES
6	400	YES
7	500	YES

At the end, all the implants were submitted to an traction until breaking effort and it was determinate the force necessary to break them.

The experimental results are systematized in table 2.

Table 2 Correlation between maximal force Fmax and displacement at Fmax

Sample	Maximal Force F max [N]	Displacement at Fmax [mm]
1	369.9	7,47
2	371.1	7,42
3	349.9	6,92
4	348.1	7,17
5	351.2	6,92
6	352.2	6,10
7	340.6	6,35

Because the tested implants are designated to mandible fractures consolidation, it was chosen a type of efforts comprised in the physiological limits of a normal mastication process.

The efforts included a traction until 200 N followed by a compression until -40 N, with a loading speed of 5 mm/min. It can be seen a breaking in two steps, due to implant's breaking in the neighborhood of a screw's hole.

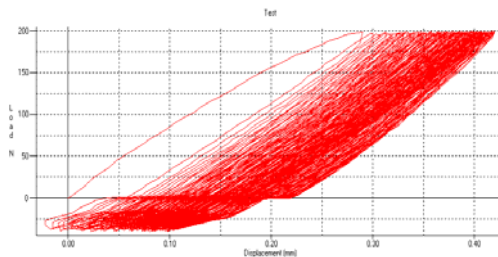


Fig. 2 - 100 cyclic efforts

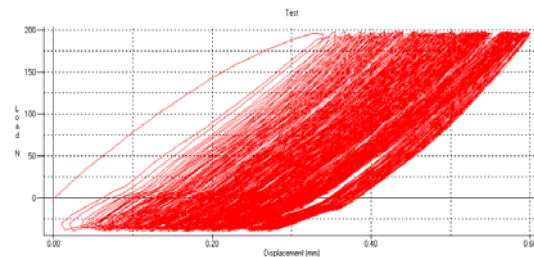


Fig. 3 - 200 cyclic efforts

The behaviour of PD6 type implants at cyclic traction efforts is represented in figures 2, 3, 4, 5.

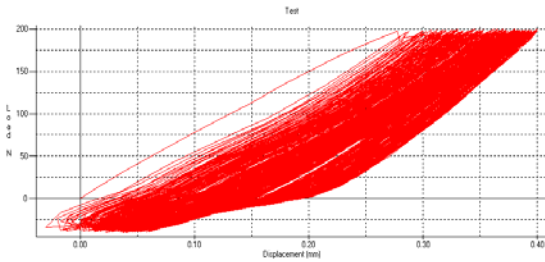


Fig. 4 - 300 cyclic efforts

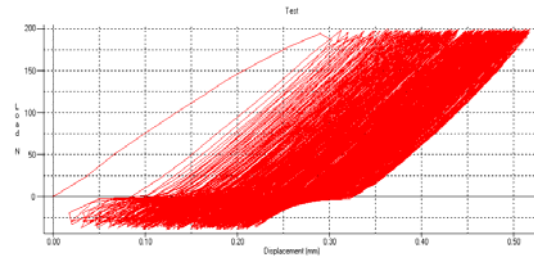


Fig. 5 - 400 cyclic efforts

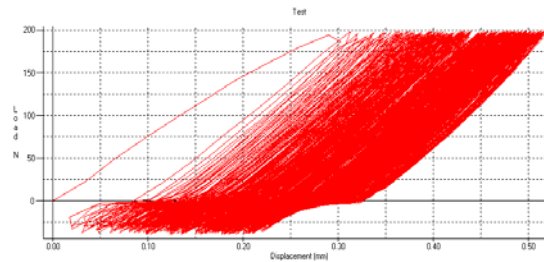


Fig. 6 - 500 cyclic efforts

The landings observed at any of these curves are caused by the clamping device, due to the conical shape of the grip. It must be mentioned that the first curve is different by the others, because it starts from 0 N, not from -40 N.

After the curves' analyse, it can be observed that the elongation at 200 N load varies, increasing proportionally with the number of cycles.

The next stage consisted in corrosion behaviour evaluation, for the samples who were the subjects of cyclic elongation efforts [7], [8].

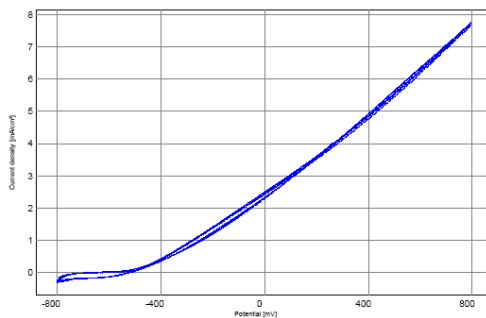


Fig. 6a Cyclic voltammetry for witness Ti sample

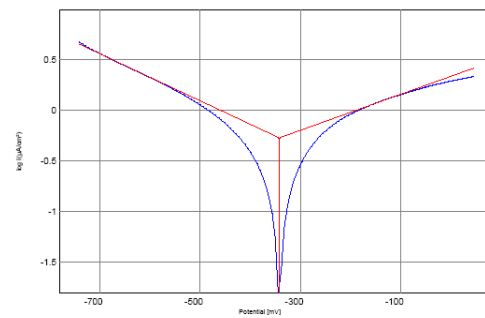


Fig. 6b Tafel representation for witness Ti sample

The curves resulted for the witness sample (which was not the subject of any traction effort) and for the cyclically solicited plates are represented in figures 6 – 8.

Experimental results:

Corrosion rate = 4,653 $\mu\text{m}/\text{year}$

$E(i=0) = -342,0 \text{ mV}$

$I_{\text{corrosion}} = 0,5342 \mu\text{A}/\text{cm}^2$

$R_p = 146,65 \text{ k}\Omega \cdot \text{cm}^2$

The corrosion rate is proportional with the area comprised between the anodic and cathodic branch of the curve. In figure 6 a it can be seen that that surface is reduced, by consequence the corrosion rate also has smaller values comparing with the other samples. The maximal potentials are displaced to more electronegative values and correspond to a smaller current density, an aspect characteristic for electrochemically stable states [6].

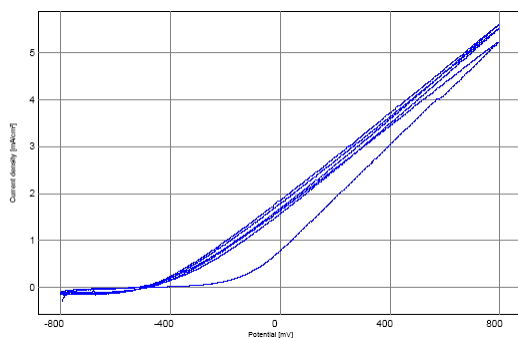


Fig. 7a Cyclic voltammetry for 100 cycles sample

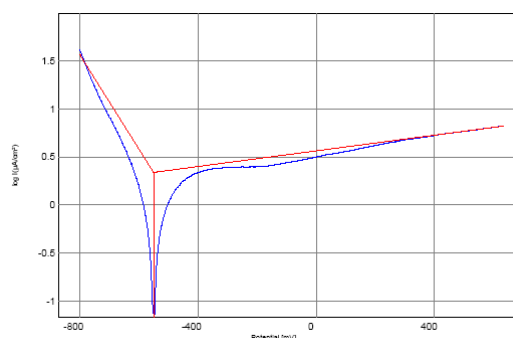


Fig. 7b Tafel representation for 100 cycles sample

Experimental results:

Corrosion rate = 19,03 µm/year

 $E(i=0) = -550,1 \text{ mV}$ $I_{\text{corrosion}} = 2,1848 \mu\text{A}/\text{cm}^2$ $R_p = 42,24 \text{ k}\Omega \cdot \text{cm}^2$

In figure 7 a can be seen that the surface comprised between anodic and cathodic branches of the curve is larger than in the previous case. The curve corresponding to the first cycle has a different allure comparing with the subsequent ones, because after the first cycle, the surface tends to stabilise. For the next two cycles it can be seen an almost perfect overlapping of the curves, for anodic and also for cathodic branches, denoting a surface stabilisation.

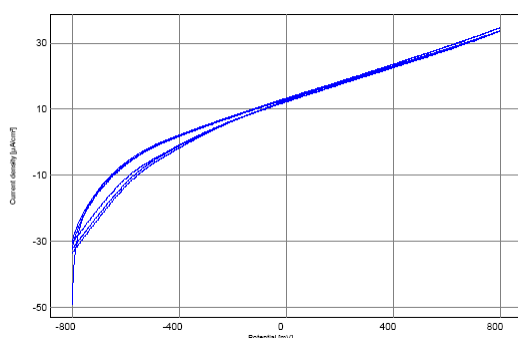


Fig. 8a Cyclic voltammetry for 200 cycles sample

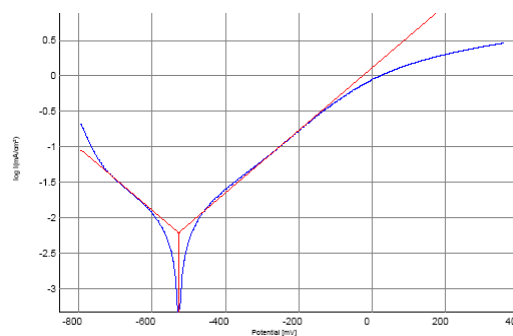


Fig.8b Tafel representation for 200 cycles sample

Experimental results:

Corrosion rate = 52,55 µm/year

 $E(i=0) = -527,4 \text{ mV}$ $I_{\text{corrosion}} = 0,0060 \text{ mA}/\text{cm}^2$ $R_p = 5,97 \text{ k}\Omega \cdot \text{cm}^2$

In figure 8 a can be seen that the surface comprised between anodic and cathodic branches presents a tendency to increase, the corrosion processes are shifting to more electronegative values, and current density is bigger than in the case of previous samples, demonstrating the presence of more intense corrosion processes. The anodic and cathodic curves are maintaining their allure. Their overlapping denotes that the corrosion process occurs with a constant rate [8].

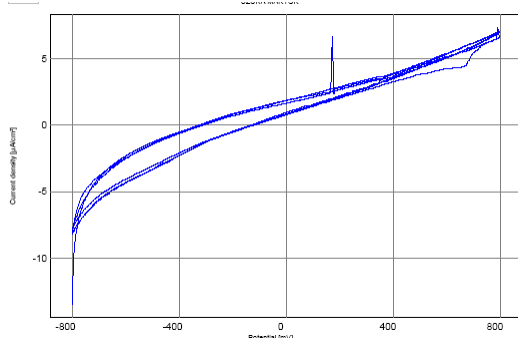


Fig. 9 a Cyclic voltammery for 300 cycles sample

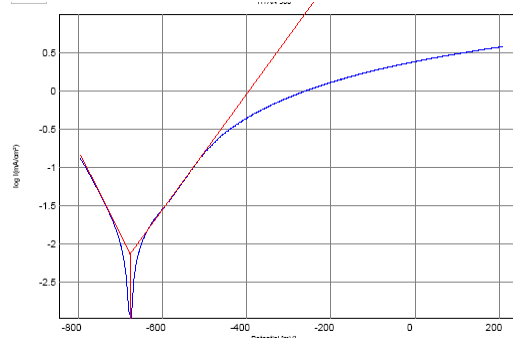


Fig. 9 b Tafel representation for 300 cycles sample

Experimental results:Corrosion rate = 63,94 $\mu\text{m}/\text{year}$ $E(i=0) = -676,3 \text{ mV}$ $I_{\text{corrosion}} = 0,0073 \text{ mA}/\text{cm}^2$ $R_p = 2,39 \text{ k}\Omega \cdot \text{cm}^2$

In figure 9 a can be seen that the surface situated under the curve is larger than in previous situations, being accompanied by an increase in current density. For the first cycle, on the curve's surface, a peak corresponding to a potential of about 200 mV and a landing comprised between 400 mV – 700 mV. These changes might be caused by a breakage of the titanium oxide protective layer, followed by its repassivation. For the next cycles, the curves' allure remains constant, denoting surface stabilization [1], [2], [3].

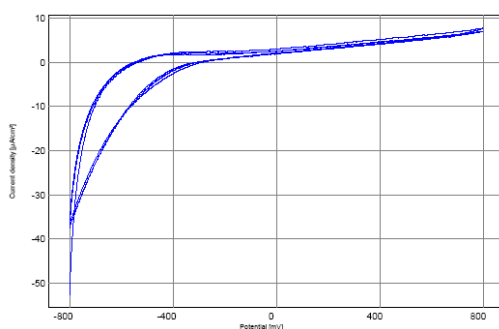


Fig. 10 a Cyclic voltammery for 400 cycles sample

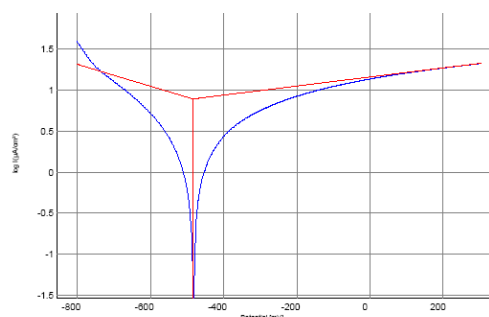


Fig. 10 b Tafel representation for 400 cycles sample

Experimental results:Corrosion rate = 68,25 $\mu\text{m}/\text{year}$ $E(i=0) = -483,0 \text{ mV}$ $I_{\text{corrosion}} = 7,8349 \mu\text{A}/\text{cm}^2$ $R_p = 27,95 \text{ k}\Omega \cdot \text{cm}^2$

In figure 10 a can be seen that the surface delimited by the curve is larger, the corrosion process is shifted to more electronegative potentials and higher current densities, corresponding to a higher corrosion rate. The anodic and cathodic branches of the curves are overlapping, demonstrating that the process occurs with a constant rate [3], [6], [7].

The experimental results are systematised in table 3.

Table 3 Experimental values

Sample	Corrosion rate [nm/an]
Witness 1	-
Corroded witness	4,653
100 cycles	19,030
200 cycles	52,550
300 cycles	63,940
400 cycles	68,250

First curve is different of the others because it was started from the value of 0 N, not – 40 N. After curves' analyse it can be seen than the elongation at 200 N load varies ascending with the increase of the number of cycles.

In the next stage, the implants were the subject of traction efforts, until breaking. The graphics resulted for the six evaluated implants are represented in figures 11 -17.

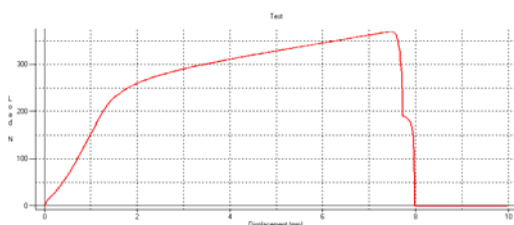


Fig.11 PD6 Plate not solicited

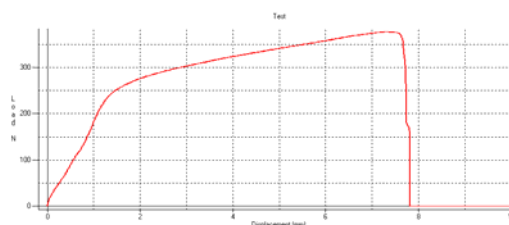


Fig.12 PD6 Plate corroded

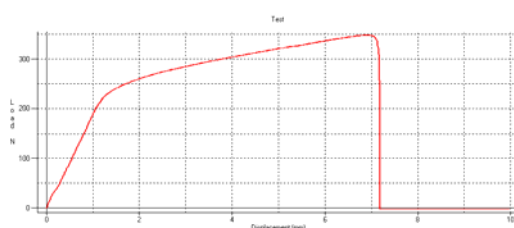


Fig.13 PD6 Plate corroded +100 cycles

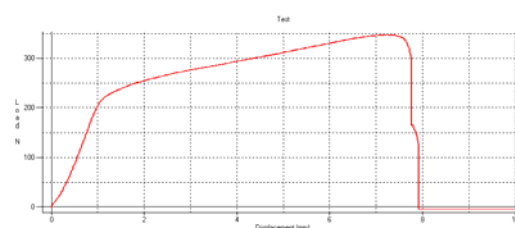


Fig.14 PD6 Plate corroded +200 cycles

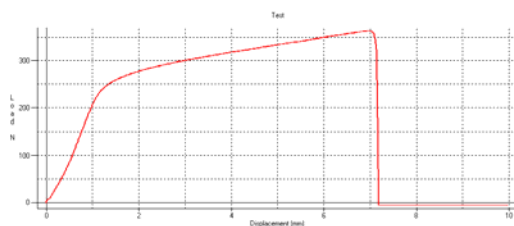


Fig.15 PD6 Plate corroded +300 cycles

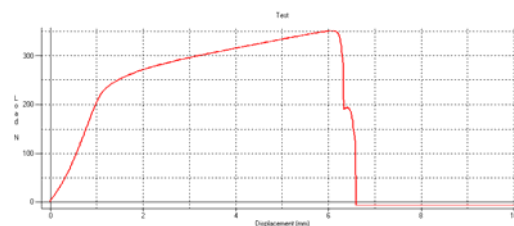


Fig. 16 PD6 Plate corroded +400 cycles

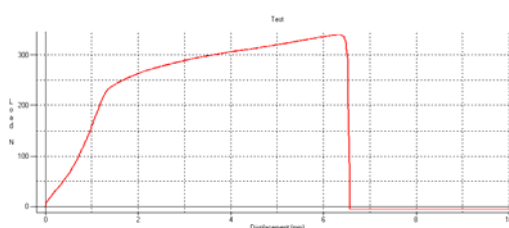


Fig. 17 PD6 Plate corroded +500 cycles

From the graphics presented above, it results than for the interval comprised between 0-1,25 mm (measured on the abrupt branch of the curve) corresponds to elastic deformation. It is almost the same for all tested plates.

On the interval correspondent to plastic deformations (1,25 mm until breaking point) graphic's slope ($\text{tg } \alpha$) is almost equal for all the samples.

Implants' elongation until break point decreases with the number of cycles, but not in a significant manner. So, for a 500 cycles solicited implant, the deformation until break point decrease with approximately 1 mm (figure 18).

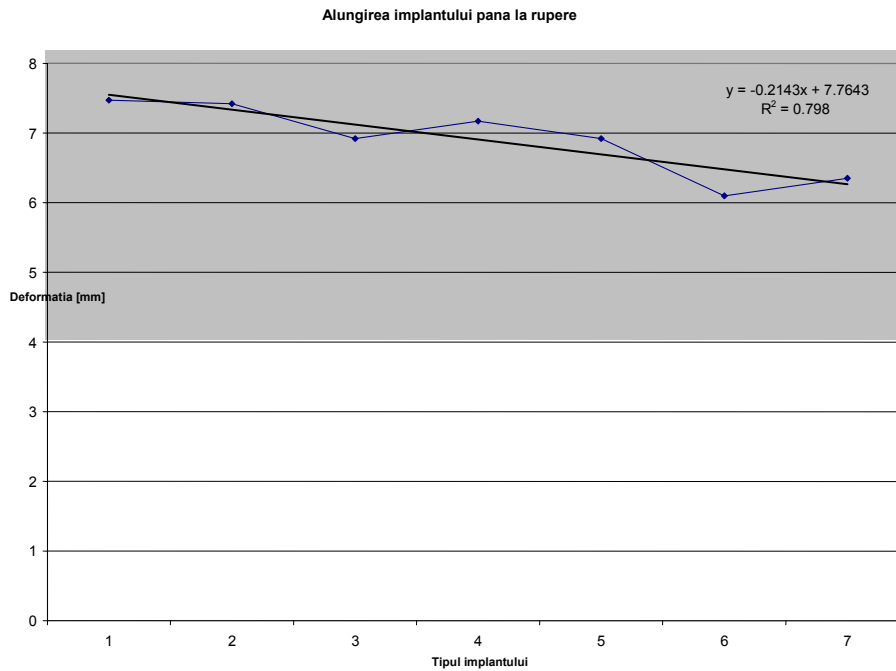


Fig. 18 Implants' elongation until break point

In figure 19 can be seen than in parallel with the increase of the number of cycles, maximal force at break point diminish, due to material's fatigue.

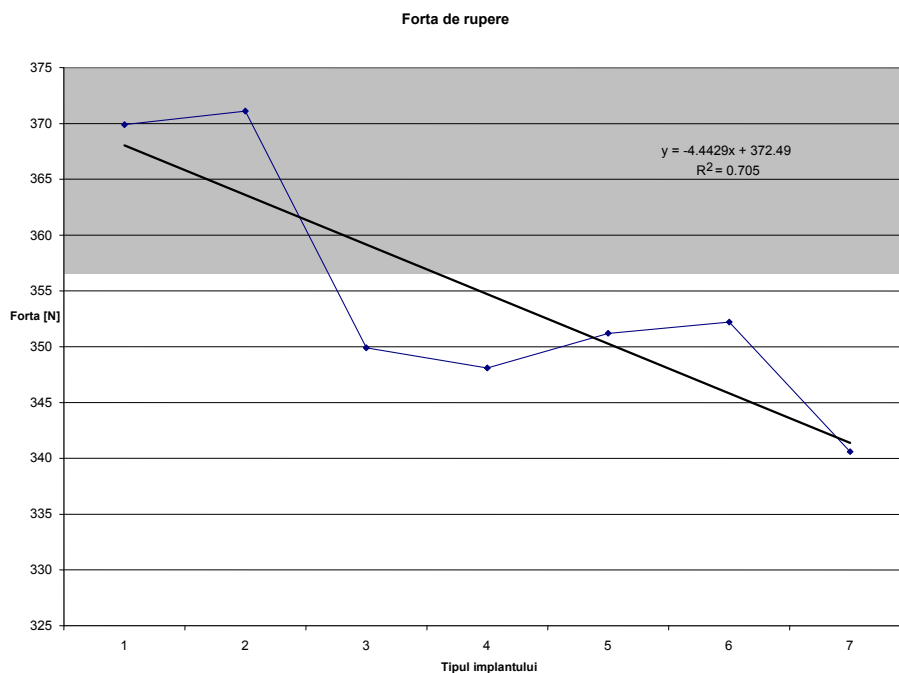


Fig. 19 Breaking force variation

In table 4 are systematized the efforts and the obtained results.

Table 4. The values obtained after the experimental determinations

Sample	F Max [N]	Elongation at F Max [mm]	Corrosion rate [nm/an]
Witness1	369,9	7,47	-
Corroded witness	371,1	7,42	4,653
100 cycles	349,9	6,92	19,030
200 cycles	348,1	7,17	52,550
300 cycles	351,2	6,92	63,940
400 cycles	352,2	6,10	68,250
500 cycles	340,6	6,35	-

3. CONCLUSIONS

After the analyze of data comprised in the table, it could be concluded than:

In this situation, corrosion doesn't significantly influence the break down force, its value being almost the same for the corroded and also for the not corroded implant. (1.2 N).

Cyclic efforts seems to have more influence over corrosion rate, increasing its values from 4,653 nm/year for the witness sample up to 68,250 nm/year in the situation of 400 cyclic efforts solicited sample.

REFERENCES

- [1] Blackwood D., Chooi S.: "*Stability of protective oxide films formed on porous titanium*", Corros. Sci., 44: 395-405, 2002
- [2] Blackwood D., Peter L., Williams D.: "*Stability and open circuit breakdown of passive films on titanium*", Electrochim. Acta, 33: 1143-1149, 1988
- [3] Blackwood D., Seah K., Teoh S.: "*Corrosion of Metallic Implants*", In: Engineering Materials for Biomedical Applications, S.H. Teoh, Published by World Scientific Publishing Co. Pte. Ltd., 2004
- [4] Echavarria A., Arroyave C.: "*Electrochemical assessment of some titanium and stainless steel implant*", Rev. Metal. Madrid Vol. Extr. 174-181, 2003
- [5] Morita M., Sasada T., Hayashi H., Tsukamoto Y., *The corrosion fatigue properties of surgical implants in a living body*, J. Biomed. Mater. Res., 22: 529-540, 1988
- [6] *** - ASTM G5-94 (2004) *Standard Reference Test Method for Making Potentiostatic and Potentiodynamic Anodic Polarization Measurements*
- [7]*** - ISO 16428: 2005 *Implants for surgery - Test solutions and environmental conditions for static and dynamic corrosion tests on implantable materials and medical devices*
- [8] Voicu, A., *Studiul biocompatibilitatii implantelor chirurgicale din aliaje de Titan in organismul uman*, Editura Politehnica Timisoara, 2007